Organic LETTERS

Letter

pubs.acs.org/OrgLett

Spirobifluorene-2,7-dicarbazole-4′-phosphine Oxide as Host for High-Performance Single-Layer Green Phosphorescent OLED Devices

Sébastien Thiery,[†] Denis Tondelier,[‡] Bernard Geffroy,[‡,§] Emmanuel Jacques,[∥] Malo Robin,[∥] Rémi Métivier,[⊥] Olivier Jeannin,[†] Joëlle Rault-Berthelot,[†] and Cyril Poriel*[,†]

[†]UMR CNRS 6226, Institut des Sciences Chimiques de Rennes, Rennes 35042 Cedex, France

[‡]UMR 7647, LPICM, École Polytechnique,91128 Palaiseau, France

[§]LICSEN, NIMBE UMR 3685, CEA Saclay, 91191 Gif Sur Yvette, France

[⊥]UMR CNRS 8531, PPSM, ENS Cachan, 94235 Cachan, France

[∥]UMR CNRS 6164, Institut d'Électronique et de Télécommunications de Rennes, Rennes 35042 Cedex, France

Supporting Information

ABSTRACT: A new host material based on the 2,7,4′-substituted spirobifluorene platform has been designed and used in single-layer phosphorescent OLED with very high efficiency (EQE = 13.2%) and low turn-on voltage (2.4 V). This performance is among the best reported for green single-layer PhOLEDs and may open new avenues in the design of host materials for single-layer devices.

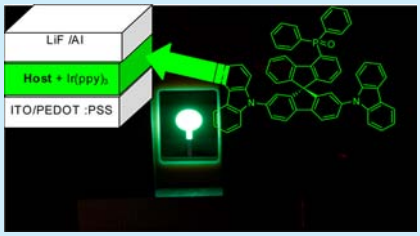

Phosphorescent organic light emitting diode (PhOLED) constitutes nowadays a very promising technology as internal quantum efficiency of 100% can be reached.[1−3] To facilitate the injection of charges and their transport, PhOLEDs are classically constituted of injecting/transporting organic layers in addition to the host−guest emitting layer (EML). On the other hand, to reach very high efficiencies, the confinement of the triplet excitons within the EML is also a key feature, which can be achieved by the addition of organic layers with a very high triplet-state energy level (E_T). Thus, a typical PhOLED is made of numerous functional organic layers, which have a key role in the device performance. Today, the layer-by-layer thermal evaporation is perfectly mastered in PhOLED technology, but the production cost remains important. Simplifying the device architecture to reach single-layer PhOLEDs would be highly beneficial to decrease the whole cost of the PhOLED. However, very high performance single-layer PhOLEDs of various colors (red,[4,5] yellow,[5−7] orange,[6−8] green,[5,6,8−10] blue,[8] and even white[11]) are very rare in the literature, and they remain an important challenge in organic electronics. This absence is due to the lack of highly efficient host materials, which must substitute all the functional organic layers in multilayer devices. Thus, the design of host materials for single-layer devices is of key importance as it should allow (i) the efficient charge injection (alignment of the HOMO/LUMO levels with the work functions of the anode and cathode respectively), (ii) an efficient charge transport (high and well-balanced mobility of charge carriers),[3] and (iii) the confinement of the triplet excitons within the EML (high E_T). Finally, the host should be synthesized through a short and efficient route, which is a key criterion for industrial production.

In this work, through a rational design, we report a new spiro-configured host material (**2,7-DiCbz-SBF-4′-POPh$_2$**, Scheme 1)

Scheme 1. Synthesis of 2,7-DiCbz-SBF-4′-POPh$_2$

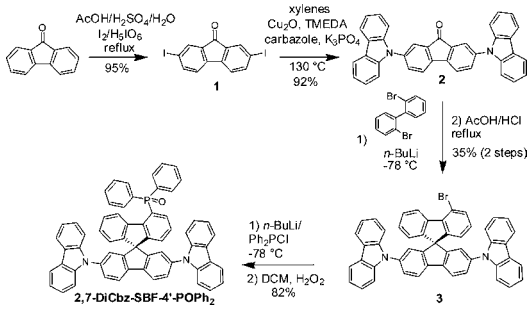

suitable for use in very high efficiency green single-layer PhOLEDs (EQE = 13.2%) with low threshold voltage (2.4 V). To the best of our knowledge, the present PhOLED performance is among the highest reported to date for green single-layer PhOLED and highlights the fantastic potential of the 4-spirobifluorene platforms, barely studied to date,[12−14] as hosts for such devices. The present molecular design is based on the connection of an electron-donating fragment (carbazole/fluorene/carbazole) and an electron-accepting fragment (phosphine oxide/fluorene), spatially separated by a spiro carbon, which is a key point to avoid a strong E_T decrease.

Received: July 15, 2015
Published: September 15, 2015

DOI: 10.1021/acs.orglett.5b02027
Org. Lett. 2015, 17, 4682−4685

The synthesis of **2,7-DiCbz-SBF-4′-POPh$_2$** was performed in four steps from commercially available 9*H*-fluorenone, which was first iodinated in C2 and C7 in the presence of I_2/H_5IO_6 (yield = 95%, Scheme 1). The efficient, copper-catalyzed Goldberg reaction was then employed to attach the carbazoles, leading to the formation of recently reported 2,7-di(9*H*-carbazol-9-yl)-9*H*-fluoren-9-one (**2**)[15] with 92% yield. A monolithium−halogen exchange on 2,2′-bromobiphenyl was then performed, and the corresponding lithiated compound was trapped with **2** leading to a fluorenol intermediate, immediately involved in an intramolecular electrophilic ring closure to provide **3** with 35% yield. One further lithium−halogen exchange on **3**, followed by the trapping of the resulting lithiated intermediate with chlorodiphenylphosphine, formed the corresponding phosphine compound, which immediately oxidized (H_2O_2) to provide **2,7-DiCbz-SBF-4′-POPh$_2$** (yield = 82%). Thus, a spirobifluorene platform substituted at C2, C7, and C4′ has been synthesized at the gram scale through an efficient and versatile synthetic approach (overall yield of 25%). It should be also mentioned that this route is a low cost approach as it does not use any Pd catalyst. In order to study the impact of the incorporation of the donor and acceptor units within **2,7-DiCbz-SBF-4′-POPh$_2$**, its properties will be compared to those of previously reported structurally related compounds: unsubstituted **SBF**,[13] **spiro-2CBP** composed of a SBF core substituted with two carbazoles in C2 and C7,[16,17] and **4-POPh$_2$-SBF** (called **SPP011** in a previous work[18]) composed of a SBF core substituted in C4 with a diphenylphosphine oxide.

From X-ray data (Figure 1, left), a 87.3° angle between the mean planes of the two central cyclopentadienyl units of spiro-

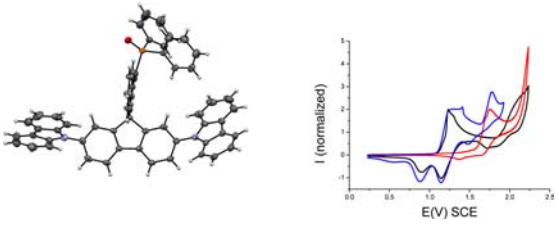

Figure 1. ORTEP drawing (left, 50% ellipsoid probability) of **2,7-DiCbz-SBF-4′-POPh$_2$** and cyclic voltammetry (Pt electrode, 100 mV/s, CH_2Cl_2 0.2 M Bu_4NPF_6, normalized on the first wave) of **2,7-DiCbz-SBF-4′-POPh$_2$** (black line), **4-POPh$_2$-SBF** (red line) and **spiro-2CBP** (blue line).

conjugated fluorenes was measured, consistent with the orthogonal configuration observed in almost all SBF derivatives (89.4° in **SBF**).[19] This means that the substitution on the C4′ position of one fluorene and on the C2/C7 positions of the other does not disturb the orthogonality of the two fluorenes. The absence of intense conjugation (see below) between these two fluorenes finds its origin in this orthogonality. On the contrary, substitution with carbazoles and diphenylphosphine oxide induces a clear deviation from planarity of the two fluorenes with deformation angles of 8.3° and 7.3° for the 4′-substituted and for the 2,7-substituted fluorene, respectively (the planarity of the fluorenes is of 1.2° and 4.2° in **SBF**).[13,19] This unusual large deformation of the 4-substituted fluorene is attributed to the steric hindrance induced by the *ortho* linkage of the C4 position.[13]

The study of the thermal properties is of great importance before any device applications can occur. The temperature of decomposition (T_d, corresponding to 5% mass loss) of **2,7-DiCbz-SBF-4′-POPh$_2$** was measured by thermogravimetric analysis and occurred at the very high temperature of 426 °C (SI), significantly higher than that of **SBF** (T_d = 234 °C)[13] and that of **4-POPh$_2$-SBF** (T_d = 297 °C, SI). However, it should be mentioned that model compound **spiro-2CBP** presents a higher T_d (587 °C),[16] meaning that the introduction of phosphine oxide on C4′ drastically drops the T_d by 160 °C. In differential scanning calorimetry, glass transition (T_g) is observed at the very high temperature of 193 °C, almost identical to that of **spiro-2CBP** (194 °C[16]) and strongly higher than those reported for **4-POPh$_2$-SBF** (127 °C[18]) and other 4-substituted SBFs.[14,20,21] This means that the substitution on the two fluorenes is highly beneficial to increase the T_g, a key feature for OLED stability.

The electrochemical properties of **2,7-DiCbz-SBF-4′-POPh$_2$**, **spiro-2CBP**, and **4-POPh$_2$-SBF** have been studied under the same experimental conditions using cyclic voltammetry (Figure 1, right). From the onset oxidation potential of both **2,7-DiCbz-SBF-4′-POPh$_2$** and **spiro-2CBP** recorded at 1.11 V (vs SCE), their HOMO levels were evaluated at −5.51 eV (HOMO = E^{onset} (vs SCE) +4.4), largely higher than that of **SBF** (−5.94 eV).[13] In light of the distribution of the HOMO level determined with density functional theory (DFT) at the Gaussian09 B3LYP/6-311+G(d,p) level of theory, the first electron transfer in oxidation is clearly assigned to the "carbazole/fluorene/carbazole" fragment (SI). **4-POPh$_2$-SBF** under the same experimental conditions displays a maximum at 1.75 V with an onset potential at 1.6 V, leading to a HOMO level of −6.00 eV (Figure 1, right). Thus, the HOMO level of **4-POPh$_2$-SBF** is very deep, even slightly deeper than that of **SBF** (−5.94 eV), clearly indicating the slight influence of the phosphine oxide on the fluorene oxidation. In the cathodic range (SI), no clear reduction wave was observed neither for **2,7-DiCbz-SBF-4′-POPh$_2$** or for **4-POPh$_2$-SBF**, and only the onset potentials have been detected at the same value of −2.30 V, allowing evaluation of their LUMO energy levels at −2.10 eV. Similarly, the LUMO of **spiro-2CBP** is evaluated at −2.00 eV (SI). In **2,7-DiCbz-SBF-4′-POPh$_2$**, it is difficult to assign with a complete certitude if this electron transfer is centered on the fluorene bearing the phosphine or on the fluorene bearing the carbazoles. Indeed, DFT calculations show that the LUMO/LUMO+2 (dispersed on the fluorene bearing the carbazoles) and LUMO+1 (dispersed on the fluorene bearing the phosphine oxide) are degenerated (SI). It should be mentioned that for **4-POPh$_2$-SBF**, the LUMO (dispersed on the phosphine oxide fluorene) and LUMO+1 (dispersed on the non substituted fluorene) are not degenerated (SI), showing the influence of the incorporation of the carbazoles on the LUMO levels. The electrochemical gaps ΔE^{el} have been evaluated at ca. 3.41 eV for **2,7-DiCbz-SBF-4′-POPh$_2$**, at ca. 3.51 eV for **spiro-2CBP**, and at ca. 3.90 eV for **4-POPh$_2$-SBF**. Important information can be deducted from the electrochemical behavior of **2,7-DiCbz-SBF-4′-POPh$_2$**: (i) its ΔE^{el} is 0.64 eV more contracted than that of **SBF** (4.05 eV)[13] and is almost identical to that of **spiro-2CBP**,[16] meaning that the main electronic properties are driven by the carbazole/fluorene/carbazole moiety, and (ii) the withdrawing effect of the phosphine oxide on the C4′ position of the fluorene remains weak due the π-conjugation disruption induced by this sterically hindered linkage and by the tetrahedral geometry of the phosphine (Table 1). As ΔE^{el} of **SBF** is of 4.05 eV, the C4′-substitution of **4-POPh$_2$-SBF** reduces the gap by only 0.15 eV (mainly by decreasing the LUMO energy level), highlighting the strong interest of this position to keep a wide gap.

The **2,7-DiCbz-SBF-4′-POPh$_2$** absorption spectrum in cyclohexane presents a shape similar to that of **spiro-2CBP**,[17] with two

DOI: 10.1021/acs.orglett.5b02027
Org. Lett. 2015, 17, 4682−4685

Table 1. Electronic Properties

	LUMO[a] (eV)	HOMO[a] (eV)	ΔE^{el}[a] (eV)	ΔE^{opt}[b] (eV)	E_T[c] (eV)
2,7-DiCbz-SBF-4′-POPh$_2$	−2.10	−5.51	3.41	3.41	2.64
spiro-2CBP	−2.00	−5.51	3.51	3.36[16]	2.64
4-POPh$_2$-SBF	−2.10	−6.00	3.90	3.75	2.78[18]
SBF[13]	−1.89	−5.94	4.05	3.97	2.87

[a]From electrochemical data. [b]From UV−vis absorption spectrum in solution in cyclohexane. [c]From emission spectrum at 77 K.

main maxima at 292 and 349 nm leading for both molecules to an almost identical optical gaps ΔE^{opt} (3.41 and 3.36 eV respectively) (Figure 2, left) in accordance with the electro-

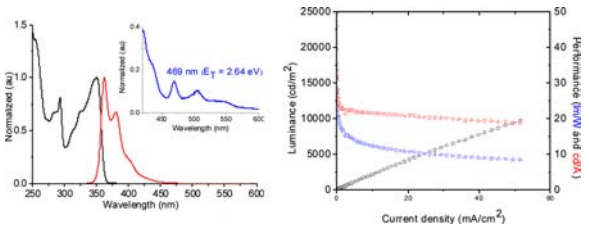

Figure 2. (Left) Absorption/emission spectra at rt (cyclohexane, λex =325 nm); inset, emission spectrum at 77 K (2-MeTHF, λex =315 nm) of **2,7-DiCbz-SBF-4′-POPh$_2$**. (Right) Luminance, current, and power efficiency as a function of current density for single-layer device (EML, **2,7-DiCbz-SBF-4′-POPh$_2$**/Ir(ppy)$_3$).

chemical gaps. These absorption bands could be attributed to optical transitions implying the longer π-conjugated fragment, namely the carbazole/fluorene/carbazole fragment. Indeed, time-dependent density functional theory (TD-DFT) calculations performed at the Gaussian09 B3LYP/6-311+G(d,p) level of theory show that the HOMO−LUMO transition possesses a large oscillator strength (f = 0.489, λ = 370.8 nm, SI) due to the significant overlap between the HOMO and LUMO/LUMO+1/LUMO+2.

2,7-DiCbz-SBF-4′-POPh$_2$ exhibits sharp and well-defined emission spectrum at room temperature (in cyclohexane) with two maxima at 362 and 380 nm (Figure 2, left). Thanks to its orthogonal and rigid structure, **2,7-DiCbz-SBF-4′-POPh$_2$** exhibits a small Stokes shift of 13 nm and a small full-width half-maximum wavelength of 31 nm. In addition, **2,7-DiCbz-SBF-4′-POPh$_2$** is a very efficient violet-blue fluorophore with a very high quantum yield of 0.78 in solution (quinine sulfate as reference) indicating few nonradiative pathways from S_1 to S_0 and still fewer intersystem crossings (ISC) from S_1 to T_1 as described below. The model compound **spiro-2CBP** presents in toluene a less structured emission spectrum and a very high quantum yield of 0.87,[17] indicating that the incorporation of the phosphine in **2,7-DiCbz-SBF-4′-POPh$_2$** does not lead to a strong increase of deactivation pathways. This has been confirmed by the radiative/nonradiative constants determined below. Indeed, the fluorescence decay curve of **2,7-DiCbz-SBF-4′-POPh$_2$** measured in cyclohexane under 300 nm laser excitation (SI) provides a lifetime of 1.21 ns, which is noticeably shorter than that of **SBF** (4.6 ns).[13] However, we note that the nonradiative constants for both molecules are in the same range; k_{nr}(**SBF**) = 1.3 × 10^8 s^{-1} vs k_{nr}(**2,7-DiCbz-SBF-4′-POPh$_2$**) = 1.8 × 10^8 s^{-1}. Thus, despite the presence of additional carbazoles and phosphine oxide in the structure of **2,7-DiCbz-SBF-4′-POPh$_2$** compared to that of **SBF**, which would allow additional nonradiative pathways in the deactivation processes of the excited states, the nonradiative constants remain interestingly similar. One can hence suggest that **2,7-DiCbz-SBF-4′-POPh$_2$** undergoes a rigidification in the excited state in accordance with its resolved emission spectrum. On the contrary, the radiative constant k_r of **2,7-DiCbz-SBF-4′-POPh$_2$** is 1 order of magnitude larger than that of **SBF**[13] (k_r(**SBF**) = 8.7 × 10^7 s^{-1} vs k_r(**2,7-DiCbz-SBF-4′-POPh$_2$**) = 6.4 × 10^8 s^{-1}), indicating that the higher quantum yield of **2,7-DiCbz-SBF-4′-POPh$_2$** compared to that of **SBF** (40%) is directly linked to this radiative constant. Finally, **2,7-DiCbz-SBF-4′-POPh$_2$** interestingly exhibits a small solvatochromic effect in fluorescence spectroscopy from 362 nm in cyclohexane to 383 nm in acetonitrile (SI), indicating a weak photoinduced intramolecular charge transfer (ICT). Since strong ICT are usually found in dyes with spatially separated HOMO/LUMO and low quantum yield,[22,23] the weak ICT of **2,7-DiCbz-SBF-4′-POPh$_2$** is in accordance with a HOMO/LUMO mixing and with the high quantum yield mentioned sabove.

Due to its high fluorescent quantum yield, the ISC is not preferred in **2,7-DiCbz-SBF-4′-POPh$_2$**, and the phosphorescence contribution at 77 K (in 2-MeTHF, Figure 2, left, inset) is very weak. Despite this, the first observable band is broad and located at 469 nm, giving an E_T value of 2.64 eV, identical to that of **spiro-2CBP** (SI) and in accordance with its use with green phosphorescent emitter Ir(ppy)$_3$ (E_T = 2.42 eV). Thus, the double substitution of the SBF core in the C2/C7 and C4′ positions and the spatial separation of the substituents via the spiro bridge only lead to an E_T decrease of 0.23 eV compared to nonsubstituted **SBF** (E_T = 2.87 eV).[13] Thus, **2,7-DiCbz-SBF-4′-POPh$_2$** is a very efficient violet-blue fluorophore and displays nevertheless a relatively high E_T, a key point to reach multifunctional materials.

The electron and hole mobility of a host strongly influences the performance of a single-layer device, and charge carrier properties of **2,7-DiCbz-SBF-4′-POPh$_2$** have been evaluated by the space charge limited current (SCLC) method. For a film thickness of 86 nm, current densities J_n and J_p are high enough to reach the SCLC regime, and we calculate a hole mobility of 8.5 × 10^{-7} cm^2/V.s (±2.1 × 10^{-7}) and an electron mobility of 4.2 × 10^{-8} cm^2/V.s (±1.2 × 10^{-8}). Thus, there is only ∼1 order of magnitude between hole and electron mobility, which is an important feature for a well charge balance within the OLED.

2,7-DiCbz-SBF-4′-POPh$_2$ was finally incorporated as host for the green phosphorescent dopant Ir(ppy)$_3$ in a single-layer PhOLED (Table 2 and Figure 2, right). Many highly efficient

Table 2. Performance of Single-Layer Device Using 2,7-DiCbz-SBF-4′-POPh$_2$ as Host

	10 mA/cm^2			max			
Von (V)	EQE (%)	CE (cd/A)	PE (lm/W)	EQE (%)	CE (cd/A)	PE (lm/W)	B cd/m^2 (J mA/cm^2)
2.4	6.2	21.5	12.4	13.2	45.8	49.6	19830 (210)

hosts for green PhOLEDs have been described in the literature for the few last years but very rarely incorporated in single-layer devices.[5,8−10] Thus, a very simple PhOLED with no transporting/blocking layer has been fabricated (ITO/PEDOT:PSS/Host:Ir(ppy)$_3$ (10%) /LiF/Al). It should be nevertheless stressed that the anode is not a neat ITO but a ITO/PEDOT:PSS anode as classically used in such devices (ITO/MoO_3 anode is also sometimes used).[5,9,11] This PhOLED displays impressively high

DOI: 10.1021/acs.orglett.5b02027
Org. Lett. 2015, 17, 4682−4685

maximal external quantum efficiency (EQE) of 13.2%, maximum luminance of ca. 20000 cd·m^{-2}, maximum current efficiency (CE) of 45.8 cd/A, and maximum power efficiency (PE) as high as 49.6 lm/W (at 0.01 mA/cm^2 and 2.9 V, Table 2). These performances appear remarkably high for a single-layer device. Even at the high luminance of 1000 cd/m^2, the device still shows a relatively high EQE of 6.4%, CE of 22.2 cd/A, and PE of 14.2 lm/W (J = 4.5 mA/cm^2). In addition, the diode starts to emit at a very low voltage of 2.4 V, highlighting the efficiency of the present host to obtain high performance single-layer PhOLED with low Von.

As mentioned previously, there are only a few examples of highly efficient single-layer green PhOLEDs reported to date. Wong and co-workers have, for example, reported in 2010 a high EQE of 7.2% for a single-layer green PhOLED.[9] As these PhOLEDs are built with the same device configuration as that described herein, the different performance can be attributed to the efficiency of the host within the device. Similarly, a very high EQE of 12.4% has been reported by Ma and co-workers with a higher threshold voltage (3 V) and a twice lower PE (27.2 lm/W) as compared to this work.[5] In order to shed light on the efficiency of the present host, we have investigated benchmark devices using **4-POPh$_2$-SBF** and **spiro-2CBP** as host (SI). First, single-layer PhOLED using **spiro-2CBP** as host displays very poor performance with an EQE of 0.3%, surely due to its very poor electron transport capability. From a chemical design point of view, one can conclude that the carbazole/fluorene/carbazole moiety, despite being strongly involved in the properties in solution, is not directly responsible for the high performance of **2,7-DiCbz-SBF-4′-POPh$_2$**-based PhOLED. On the contrary, single-layer PhOLED using **4-POPh$_2$-SBF** as host surprisingly displays an EQE as high as that of **2,7-DiCbz-SBF-4′-POPh$_2$**-based PhOLED, i.e., 13.3%, clearly highlighting the strong influence of the phosphine oxide fragment in the PhOLED performance. However, due to the deep HOMO level of **4-POPh$_2$-SBF** (−6.00 eV), the single-layer PhOLED displays a high turn of voltage of 3.3 V, ca. 1 V higher than that using **2,7-DiCbz-SBF-4′-POPh$_2$** as host (HOMO level: −5.53 eV). This feature clearly indicates a better charge injection in the latter, which is a key point for low consumption devices. **4-POPh$_2$-SBF** is also strongly less stable than **2,7-DiCbz-SBF-4′-POPh$_2$**, as a function of the current density and the maximum luminance reached by **4-POPh$_2$-SBF**, ca. 15000 cd/m^2, is 25% lower than that of **2,7-DiCbz-SBF-4′-POPh$_2$** (20000 cd/m^2).

In summary, we have designed and synthesized, via an efficient approach, a promising host based on phosphine oxide/carbazole association on a 2,7,4′-spirobifluorene platform. Single-layer green PhOLED displays a very high EQE of 13.2% (CE = 45.8 cd/A and PE = 49.6 lm/W) with a low Von of 2.4 V, showing that the molecular design of the host fulfills the criteria required for high efficiency single-layer PhOLED. This performance is, to the best of our knowledge, among the best reported to date for green single-layer PhOLEDs and may open new avenues in the design of highly efficient materials for single-layer devices.

■ ASSOCIATED CONTENT

Supporting Information

The Supporting Information is available free of charge on the ACS Publications website at DOI: 10.1021/acs.orglett.5b02027.

Experimental section, structural/thermal/electrochemical properties, theoretical modeling, device data, 2D NMR studies, and NMR spectra (PDF)

■ AUTHOR INFORMATION

Corresponding Author

*E-mail: cyril.poriel@univ-rennes1.fr.

Notes

The authors declare no competing financial interest.

■ ACKNOWLEDGMENTS

We thank CDIFX and CRMPO (Rennes), GENCI for allocation of computing time (project c2015085032), the ISA (Villeurbanne), the Service de Microanalyse-CNRS (Gif sur Yvette), and the ANR (No. 11-BS07-020-01) for financial support and for a studentship (S.T.).

■ REFERENCES

(1) Forrest, S. R.; Baldo, M. A.; O'Brien, D. F.; You, Y.; Shoustikov, A.; Sibley, S.; Thompson, M. E. *Nature* **1998**, *395*, 151.
(2) Baldo, M. A.; O'Brien, D. F.; Thompson, M. E.; Forrest, S. R. *Phys. Rev. B: Condens. Matter Mater. Phys.* **1999**, *60*, 14422.
(3) Yook, K. S.; Lee, J. Y. *Adv. Mater.* **2012**, *24*, 3169.
(4) Hung, W.-Y.; Tsai, T.-C.; Ku, S.-Y.; Chi, L.-C.; Wong, K.-T. *Phys. Chem. Chem. Phys.* **2008**, *10*, 5822.
(5) Qiao, X.; Tao, Y.; Wang, Q.; Ma, D.; Yang, C.; Wang, L.; Qin, J.; Wang, F. *J. Appl. Phys.* **2010**, *108*, 034508.
(6) Chen, C.-H.; Huang, W.-S.; Lai, M.-Y.; Tsao, W.-C.; Lin, J. T.; Wu, Y.-H.; Ke, T.-H.; Chen, L.-Y.; Wu, C.-C. *Adv. Funct. Mater.* **2009**, *19*, 2661.
(7) Lai, M.-Y.; Chen, C.-H.; Huang, W.-S.; Lin, J. T.; Ke, T.-H.; Chen, L.-Y.; Tsai, M.-H.; Wu, C.-C. *Angew. Chem., Int. Ed.* **2008**, *47*, 581.
(8) Liu, Y.; Cui, L.-S.; Xu, M.-F.; Shi, X.-B.; Zhou, D.-Y.; Wang, Z.-K.; Jiang, Z.-Q.; Liao, L. S. *J. Mater. Chem. C* **2014**, *2*, 2488.
(9) Hung, W.-Y.; Wang, T.-C.; Chiu, H.-C.; Chen, H.-F.; Wong, K.-T. *Phys. Chem. Chem. Phys.* **2010**, *12*, 10685.
(10) Huang, B.; Jiang, W.; Tang, J.; Ban, X.; Zhu, R.; Xu, H.; Yang, W.; Sun, Y. *Dyes Pigm.* **2014**, *101*, 9.
(11) Yin, Y.; Piao, X.; Wang, Y.; Liu, J.; Xu, K.; Xie, W. *Appl. Phys. Lett.* **2012**, *101*, 063306.
(12) Romain, M.; Thiery, S.; Shirinskaya, A.; Declairieux, C.; Tondelier, D.; Geffroy, B.; Jeannin, O.; Rault-Berthelot, J.; Métivier, R.; Poriel, C. *Angew. Chem., Int. Ed.* **2015**, *54*, 1176.
(13) Thiery, S.; Tondelier, D.; Declairieux, C.; Seo, G.; Geffroy, B.; Jeannin, O.; Rault-Berthelot, J.; Métivier, R.; Poriel, C. *J. Mater. Chem. C* **2014**, *2*, 4156.
(14) Thiery, S.; Tondelier, D.; Declairieux, C.; Geffroy, B.; Jeannin, O.; Métivier, R.; Rault-Berthelot, J.; Poriel, C. *J. Phys. Chem. C* **2015**, *119*, 5790−5805.
(15) Mangione, M. I.; Spanevello, R. A. *Tetrahedron Lett.* **2015**, *56*, 465.
(16) Usluer, O.; Demic, S.; Egbe, D. A.; Birckner, E.; Tozlu, C.; Pivrikas, A.; Ramil, A. M.; Saricifci, N. S. *Adv. Funct. Mater.* **2010**, *20*, 4152.
(17) Nakanotani, H.; Akiyama, S.; Ohnishi, D.; Moriwake, M.; Yahiro, M.; Yoshihara, T.; Tobita, S.; Adachi, C. *Adv. Funct. Mater.* **2007**, *17*, 2328.
(18) Jang, S. E.; Joo, C. W.; Jeon, S. O.; Yook, K. S.; Lee, J. Y. *Org. Electron.* **2010**, *11*, 1059.
(19) Schenk, H. *Acta Crystallogr., Sect. B: Struct. Crystallogr. Cryst. Chem.* **1972**, *28*, 625.
(20) Dong, S.-C.; Gao, C.-H.; Zhang, Z.-H.; Jiang, Z.-Q.; Lee, S.-T.; Liao, L. S. *Phys. Chem. Chem. Phys.* **2012**, *14*, 14224.
(21) Fan, C.; Chen, Y.; Gan, P.; Yang, C.; Zhong, C.; Qin, J.; Ma, D. *Org. Lett.* **2010**, *12*, 5648.
(22) Romain, M.; Tondelier, D.; Geffroy, B.; Shirinskaya, A.; Jeannin, O.; Rault-Berthelot, J.; Poriel, C. *Chem. Commun.* **2015**, *51*, 1313.
(23) Romain, M.; Tondelier, D.; Geffroy, B.; Jeannin, O.; Jacques, E.; Rault-Berthelot, J.; Poriel, C. *Chem. - Eur. J.* **2015**, *21*, 9426−9439.

DOI: 10.1021/acs.orglett.5b02027
Org. Lett. 2015, 17, 4682−4685